Understanding Concurrent Transmissions over Ultra-Wideband Complex Channels

Maximilian Schuh
schuh@tugraz.at
Graz University of Technology
Graz, Austria

Michael Baddeley
Michael.Baddeley@tii.ae
Technology Innovation Institute
Abu Dhabi, United Arab Emirates

Kay Römer
roemer@tugraz.at
Graz University of Technology
Graz, Austria

Carlo Alberto Boano
cboano@tugraz.at
Graz University of Technology
Graz, Austria

ABSTRACT

Ultra-wideband (UWB) devices operate only on a few frequency channels and commonly lack clear channel assessment capabilities: this makes it difficult to support several devices operating concurrently within a single network or to avoid coexistence issues with other UWB-based systems operating in close proximity. To address this issue, the IEEE 802.15.4 standard proposes the use of *complex channels* (i.e., diverse combinations of frequency channels and preamble codes) to enable multiple orthogonal transmissions. However, existing studies have shown that concurrent UWB transmissions on different complex channels are unreliable and incur high packet loss. In this paper, we investigate and shed light on the reason for this packet loss. We then present concrete methods to boost the reliability of concurrent UWB communications over different complex channels and demonstrate their effectiveness experimentally. In detail, we show that the synchronization and clock frequency offset among concurrent transmitters as well as the employed physical layer settings can be used to increase communication performance over different complex channels. Our study shows the feasibility of more than eight concurrent UWB transmissions on the same frequencies, sustaining a packet reception rate above 99 % while retaining the ability to carry out centimetre-accurate ranging.

CCS CONCEPTS

• **Networks** → *Location based services*; *Network reliability*; *Link-layer protocols*; • **Computer systems organization** → *Embedded and cyber-physical systems.*

KEYWORDS

UWB, IEEE 802.15.4a/z, Complex channels, Coexistence, Reliability, Scalability, Clock detuning, Clock frequency offset, PHY settings, Experimentation.

SENSYS '24, November 4–7, 2024, Hangzhou, China

ACM ISBN 979-8-4007-0697-4/24/11
https://doi.org/10.1145/3666025.3699372

ACM Reference Format:
Maximilian Schuh, Michael Baddeley, Kay Römer, and Carlo Alberto Boano. 2024. Understanding Concurrent Transmissions over Ultra-Wideband Complex Channels. In *The 22nd ACM Conference on Embedded Networked Sensor Systems (SENSYS '24), November 4–7, 2024, Hangzhou, China.* ACM, New York, NY, USA, 14 pages. https://doi.org/10.1145/3666025.3699372

1 INTRODUCTION

Ultra-wideband (UWB) has recently become one of the reference technologies to build location-aware Internet of Things (IoT) applications, and its integration into modern vehicles and smartphones has led to a rapidly increasing number of UWB devices on the market [1, 42]. UWB-based smart access and keyless entry systems have indeed become ubiquitous [20, 38], along with UWB-based services for robot navigation [40, 64] and social interaction tracking [6, 36].

Dealing with concurrent operations. The proliferation of UWB devices and their growing popularity increase the need to *scale up* UWB systems so that they can support – within a single network – *hundreds to thousands* of devices frequently communicating with each other (e.g., in the context of real-time positioning and tracking in manufacturing and logistics [50, 55]). This entails the ability to coordinate the UWB devices in the network, so that they can operate (i.e., exchange data, perform ranging) *concurrently* without sacrificing performance. At the same time, one also need to *coexist* with other UWB systems co-located in the same physical space [43], which is hard among independent networks.

Table 1: UWB channels and regulatory limitations.

	IEEE 802.15.4 UWB channel															
	1 GHz	3 – 4.75 GHz				6 – 10.25 GHz										
	0	1	2	3	4	5	6	7	8	9	10	11	12	13	14	15
UWB radio																
DW1000 [18]		✓	✓	✓	✓	✓		✓								
DW3000 [19]						✓				✓						
SR040 [48]						✓	✓		✓	✓						
SR150 [49]						✓	✓		✓	✓						
U100 [51]						✓				✓						
U1 [63]						✓				✓						
Regulatory																
Europe		~	~	~	~	✓	✓	✓	✓	✓	✓					
Korea & Japan		~	~	~	~				✓	✓	✓	✓	✓	✓	✓	✓
China						✓	✓	✓	✓	✓	✓					
USA		✓	✓	✓	✓	✓	✓	✓	✓	✓	✓	✓	✓	✓	✓	✓

~ Limited access using low duty cycle or "detect-and-avoid" techniques.
Channels prone to cross-technology interference with Wi-Fi devices.

In traditional wireless systems, collisions across co-located devices transmitting concurrently are commonly avoided by using carrier sense multiple access (CSMA) techniques, by allocating non-overlapping time-slots for transmission (i.e., using TDMA schemes), and/or by configuring the devices to use distinct frequency channels (i.e., using FDMA schemes).

UWB-specific limitations. Unfortunately, *CSMA techniques cannot be easily implemented in UWB systems*, as the low signal energy makes it hard to perform energy detection, and as off-the-shelf UWB devices do not offer alternative clear channel assessment (CCA) methods [10]. Moreover, *the number of frequency channels available for UWB systems is very limited.* In fact, whilst the IEEE 802.15.4 standard defines up to 16 UWB channels, only a subset of these are usable in practice. On the one hand, off-the-shelf UWB transceivers commonly support only a few channels, as shown in Tab. 1. This is due to the inherent complexity of supporting many channels with a large bandwidth. For example, the Qorvo DW1000 – one of the first UWB radios, and still one of the most widely-used chips in research and in commercial products – supports only six out of 16 channels. Modern off-the-shelf UWB transceivers (such as the Qorvo DW3000, NXP SR150, and Apple U1) support only two or four channels. On the other hand, as also shown in Tab. 1, the number of UWB channels available for worldwide use is limited by regulatory constraints [12, 22], imposing duty cycle restrictions or enforcing interference avoidance techniques (such as "detect-and-avoid") that have not been implemented in off-the-shelf UWB transceivers yet. Several UWB channels also overlap with the frequencies used by Wi-Fi 6E and Wi-Fi 7 devices, and are hence likely to experience high packet loss [7, 53]. As a result, to ensure global acceptance and interoperability across platforms, UWB systems often need to operate on channels 5 and 9 only. This limits the frequency diversity across co-located UWB systems, and makes it hard to schedule concurrent activities within the same large-scale network using TDMA schemes [60]. The latter, in fact, are unsuitable for UWB networks with a large number of devices [3, 50].

Complex channels to the rescue? To cope with these limitations and enable multiple UWB transmissions on the same frequency channel, the IEEE 802.15.4 standard [31] outlines the concept of *complex channels*, i.e., a combination of frequency channels and preamble codes (see § 2). While the use of preamble codes sent with *different pulse repetition frequency (PRF)* allows non-interfering concurrent transmissions on the same frequency [16, 62], only three different PRFs are defined by the standard, and only few of them are implemented by off-the-shelf radios (mainly due to the reduced reliability [29] and ranging performance [44] of the lower PRFs). The use of different preamble codes sent with *the same PRF* should also allow non-interfering concurrent transmissions on the same frequency channel [31]. However, this is not true in practice, as reported by Qorvo [16, 18], and as demonstrated by Vecchia et al. [62], who reported packet loss rates between 42 % and 53 % when two concurrent transmitters employ preamble codes having the same PRF. Therefore, concurrent transmissions over different complex channels may still interfere and lead to high packet loss, unless the employed preamble codes have different PRFs.

The gap to fill. This state of affairs is problematic: the lack of frequency channels, the few PRFs available, and the insufficient reliability of complex channels when using preamble codes sent with the same PRF, hinder the design of scalable UWB systems and hampers coexistence. However, we argue that the full potential of complex channels *has not been harnessed yet.* The limited research on the topic [3, 62] has only investigated the performance of complex channels in a few scenarios, on a limited set of physical layer (PHY) settings, or using a small number of concurrent transmitters.

Our contributions. This paper presents a detailed experimental study on the reliability of concurrent UWB transmissions over several complex channels, and proposes concrete methods to effectively improve their performance. To get a better understanding of how concurrent transmissions on different complex channels perform, we carry out a large experimental campaign on a real-world testbed, in which we examine the packet loss rate and signal quality of concurrent transmissions across several test scenarios as a function of various low-level configurations and PHY settings. This allows us to confirm and generalize earlier findings, e.g., that a *tight synchronization* across concurrent transmitters increases reliability [62]. Moreover, we identify *clock detuning* and *fine-tuning of PHY settings* as levers to further improve communication performance.

We then leverage our findings to derive concrete device configurations enabling several co-located UWB devices to reliably transmit data simultaneously despite using preamble codes sent with the same PRF. We demonstrate experimentally that some of these configurations enable more than eight concurrent UWB transmissions on the same frequencies sustaining a packet reception rate (PRR) above 99 %, significantly advancing the state of the art. We further show that our proposed configurations do not affect the accuracy and precision of ranging measurements, i.e., that they can be used to improve and scale up UWB systems while retaining their ability to carry out centimetre-accurate ranging. Hence, our work enables the design of large-scale UWB systems and maximizes the coexistence across co-located devices.

Paper outline. After introducing UWB technology and complex channels (§ 2), we describe our experimental setup (§ 3) and show empirically the importance of synchronizing concurrent transmitters (§ 4), fine-tuning PHY settings (§ 5), and detuning the clock so to introduce a clock frequency offset across transmitters (§ 6). We then distil our findings and derive concrete device configurations, evaluating their scalability and impact on ranging (§ 7). We conclude the paper after discussing open challenges (§ 8) and related work (§ 9).

2 PRIMER ON UWB COMPLEX CHANNELS

This section introduces key aspects of UWB technology (§ 2.1) and illustrates the concept of *complex channels* (§ 2.2).

2.1 The IEEE 802.15.4 UWB PHY

Support for high rate pulse repetition frequency (HRP)-UWB PHY was added to the standard for low-power wireless personal area networks in 2007 as part of the IEEE 802.15.4a amendment [30]. UWB's large channel bandwidth provides a high timing resolution, enabling an accurate estimation of the time-of-flight (ToF) and hence of the distance between devices. The IEEE 802.15.4z amendment released in 2020 enhances the existing UWB PHYs with higher data rates, improved security, and increased robustness [54].

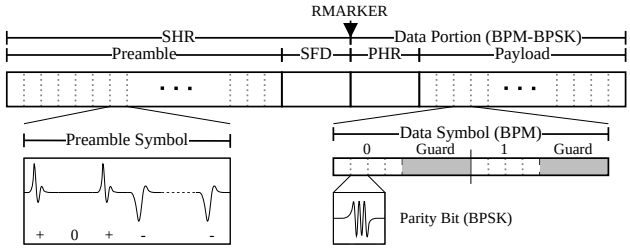

Figure 1: Structure of a UWB frame [30].

UWB frame structure. Fig. 1 illustrates the high-level structure of an IEEE 802.15.4-compliant UWB frame. Each frame starts with a *synchronization header (SHR)* consisting of a *preamble* (i.e., a repeating sequence of preamble symbols), as well as a *start-of-frame-delimiter (SFD)*. A preamble symbol is roughly 1 µs long and is built as a sequence of pulses drawn from a ternary alphabet (-1, 0, 1), corresponding to a positive, absent, or negative pulse, respectively. The sequence of pulses of a preamble symbol is called *preamble code* (detailed in § 2.2). The SFD marks the end of the SHR and the start of the data portion. The time at which the first symbol after the SFD is received, called RMARKER, is used to calculate the ToF.

Each frame's *data portion* consists of a physical layer header (PHR) and a payload. The PHR contains general information about the transmitted frame, such as its length, preamble duration, and the used data rate. The integrity of the PHR is secured using six single-error correction, double-error detection (SECDED) bits. Within the payload, 127 bytes of data can be transmitted, including two cyclic redundancy check (CRC) bytes at the end of the frame. In addition to the CRC, a forward error correction (FEC) scheme uses Reed-Solomon codes to ensure the integrity of the data portion. Within the data portion of a UWB frame, information is encoded using burst position modulation (BPM), and a parity bit is encoded using binary-phase shift keying (BPSK).

PHY settings. Off-the-shelf UWB radios offer the ability to fine-tune performance by varying several PHY settings [29, 44]. We give next an overview of the most relevant ones.

Preamble symbol repetitions (PSR). The length of the preamble within the SHR is variable and determined by the PSR. While the standard foresees four possible PSR (16, 64, 1024, or 4096), off-the-shelf UWB transceivers may support additional ones (e.g., the Qorvo DW1000 enables the transmission of preambles with a length of 128, 256, or 512 preamble symbols).

Mean pulse-repetition frequency (PRF). The mean PRF determines the average frequency at which UWB pulses are transmitted. The standard originally defined three PRFs: 4, 16, and 64 MHz, with the IEEE 802.15.4z amendment introducing also PRFs of 124.8 and 249.6 MHz. The Qorvo DW1000 and DW3000 radios only support PRFs of 16 and 64 MHz.

Data rate. The data portion (PHR and payload) can be transmitted at a data rate of either 110 kbit/s, 850 kbit/s, 6.8 Mbit/s or 27.24 Mbit/s. Notably, the default data rate for the PHR is 850 kbit/s. Only when choosing the lower data rate for the payload (110 kbit/s), also the PHR will be sent at this speed.

SFD sequence. The code for the SFD is derived from a ternary sequence folded with the selected preamble code. The chosen data rate determines the length of the SFD sequence. For the low data rate of 110 kbit/s, the sequence consists of 32 symbols, whereas the higher data rates use a short, 8-symbols sequence. The IEEE 802.15.4z standard defines additional SFD sequences [33] that do not contain zero values and have lengths of up to 32 symbols: this shall improve the signal energy (and, therefore, the robustness) of the SFD [19].

CIR estimate. During preamble reception, coherent UWB radios such as the DW1000 estimate a channel impulse response (CIR). The latter yields information about the channel properties, which can be used to evaluate the signal's quality and suitability for ranging [45]. The CIR can also be used to resolve multi-path [27], detect non-line-of-sight conditions [25], and enable concurrent ranging [13, 14, 28].

2.2 UWB Complex Channels

The IEEE 802.15.4a amendment introduces the concept of *complex channels* to increase the number of orthogonal channels for the transmission of UWB frames. A complex channel combines a frequency channel and a *preamble code*.

Preamble code. A preamble code is a sequence drawn from a ternary alphabet. The codes are designed following the Ipatov construction for perfect ternary sequences [35] and hence have an ideal periodic auto-correlation property allowing to resolve the channel accurately. The standard defines 24 preamble codes: 8 codes (1–8) of length 31 are defined for the 16 MHz PRF, while 16 codes (9–24) of length 127 are intended for the 64 MHz PRF. Even though preamble codes are meant to have a low cross-correlation among each other [32], this does still not allow a clear separation of complex channels as envisaged by the standard, according to Qorvo [18].

Empirical studies. To date, only a few works have characterized the performance of concurrent UWB communications over different complex channels experimentally.

Different PRF. The use of preamble codes with different PRFs yields truly-orthogonal transmissions on the same UWB frequency channel. Experiments using two concurrent transmitters using a PRF of 16 MHz and 64 MHz have shown high communication reliability [16, 62]. This triggered the adoption of PRF-based channel separation in time slotted channel hopping (TSCH) implementations for UWB [10, 11]. Unfortunately, off-the-shelf UWB radios typically support only two PRFs or do not implement the lower PRFs [48, 49], practically hindering a PRF-based channel separation.

Same PRF. Flury et al. [24] have simulated two co-located UWB transmitters using different preamble codes with the same PRF, showing a severe degradation of the PRR even at low traffic. Vecchia et al. [62] have been the first to confirm this on real hardware. Specifically, they set up two pairs of devices exchanging data concurrently on two complex channels, and track the PRR on both links while varying the synchronicity of the two transmitters. They report a mean PRR of 42–53%, and mention that the likelihood of both transmissions being successful is highest when frames are synchronized within a few μs. Synchronizing transmissions, however, is not always possible (e.g., in the presence of co-located UWB systems). Hence, this seminal study confirms Qorvo's statement [18] and highlights the urgent need of methods to increase the reliability of concurrent transmissions over different complex channels when using preamble codes sent with the same PRF [62].

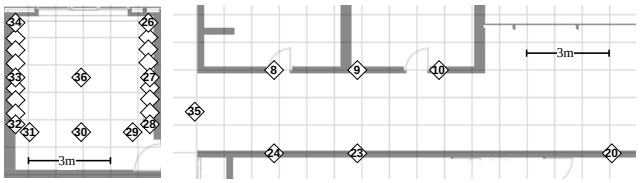

(a) OFFICE (b) HALLWAY

Figure 2: UWB devices deployed within the testbed.

3 EXPERIMENTAL METHODOLOGY

We aim to identify such effective methods improving the reliability of concurrent UWB communications. To this end, we carry out a comprehensive experimental campaign on a real-world testbed spanning several scenarios and various low-level configurations. Besides studying performance as a function of the synchronization across transmitters as previous work (§ 4), we investigate the impact of various PHY settings (§ 5), and different carrier frequency offsets (CFOs) among transmitters (§ 6). This campaign will prove crucial in identifying the sought methods to improve performance (§ 7).

Hardware. We run our measurements in a testbed consisting of 29 UWB devices deployed inside an office and across a hallway of a university building [53], covering an area of ≈207 m^2, as shown in Fig. 2. All devices are Qorvo DWM1001C-DEV boards and are mounted on a metal rail placed at a height of 2.7 m from the ground. These boards consist of a Qorvo DW1000 radio [18] attached to a Nordic nRF52832 MCU [47] and come factory-calibrated in terms of transmission power and antenna delay.

Test procedure. Our measurements build upon and extend those by Vecchia et al. [62]. To establish synchronization among multiple transmitters (which is necessary to test concurrent transmissions), we configure the UWB devices to operate in three distinct roles: initiator, sender, and receiver. In our setup, we employ a single initiator and several pairs of devices consisting of one sender and one receiver each, with each pair operating on a different complex channel. The initiator (INIT) periodically broadcasts beacon frames on a pre-defined control channel. Surrounding devices listen for these beacons, calculate their relative CFO to the initiator using the values in the carrier recovery integrator register, and use the trimming feature of the radio[1] to adjust their clock frequency so to match a pre-defined CFO γ. The surrounding devices then switch to their designated complex channel and act as either sender (TX) or receiver (RX). Senders use the delayed transmission feature of the DW1000 radio [18] to align their transmissions to the same instant I_{send}: this results in UWB frames being sent concurrently over different complex channels[2]. To vary the level of synchronization among senders, a transmission delay $\delta \in [-60, +60]$ μs is applied to I_{send} in steps of 5 µs (or of 1 µs within the interval ±20 µs). Each frame has a fixed length of 120 bytes: the first 18 bytes contain node address, message type, and a sequence number; the remaining bytes are generated randomly[3]. The RX devices listen for frames sent by the paired TX device, measure the corresponding PRR, and log debug info such as receiver failures, noise, and signal power.

[1]The clock frequency of the Qorvo DW1000 radio can be tuned in steps of roughly 1.5 ppm via the *crystal trim register* in a ±20 ppm range [18].

[2]We use a fixed delay of 2 ms between the RMARKER of the beacon sent by the INIT device and the RMARKER of the frame sent by each TX device: this ensures that both TX and RX devices have sufficient time to configure their radio and to send frames with up to 1024 preamble symbol repetitions.

Table 2: PHY settings used in the BASE configuration.

Preamble symbol repetitions (PSR)	64
Pulse repetition frequency (PRF)	64 MHz
Data Rate	6.8 Mbps
SFD sequence	IEEE 802.15.4a (8 symbols)
Preamble code	9 and 10

Metrics. At each RX device, we study the PRR and the quality of the received signal. The latter is computed as Amplitude to Noise Ratio (ANR), i.e., as the ratio between the first path amplitude (A_{fp}) and the maximum noise amplitude (A_{noise}) of the CIR. After retrieving A_{fp} and A_{noise} from the DW1000's RX_FQUAL register, we compute $ANR = A_{fp}/A_{noise}$. Note that the PRR is linked to the reliability of communication; the ANR is proportional to the ranging quality [45].

Measurement scenarios. We perform our experiments in several scenarios, each using a subset of the UWB devices in our testbed. First, we focus on four scenarios in which two pairs of TX/RX devices operate concurrently, as depicted in Fig. 3. This allows us to characterize the performance of each device pair (i.e., TX→RX link) as a function of different node placements and signal-to-interference ratios (§ 4 – § 6). We then focus on a scenario in which up to 9 pairs of devices operate concurrently, as shown in Fig. 19 (§ 7).

PHY settings. We run all our measurements on channel 5 due to its availability on most off-the-shelf UWB radios (see Tab. 1). We also use a PRF of 64 MHz, as lower PRFs are known to perform worse [29, 62] and are often not available in newer radios. Unless otherwise stated, we use a default configuration (BASE, summarized in Tab. 2) in which devices employ 64 PSR, a data rate of 6.8 Mbps, an 8-symbols SFD sequence, and adjust their CFO to γ=0 ppm. For the pairs of devices shown in Fig. 3, we use preamble code 9 for the first link (*link 1*, red, dashed) and 10 for the second (*link 2*, blue, dotted). For each measurement, every TX sends 2000 packets.

4 BENEFITS OF SYNCHRONIZATION

We next study how the level of synchronization among senders affects the reliability of concurrent transmissions. We expect that a tight synchronization across concurrent transmitters helps increasing performance. In fact, Vecchia et al. [62] studied the reliability of two pairs of devices transmitting concurrently on channel 4 with a fixed PSR of 128 in two different scenarios, observing a PRR between 42 % and 53 %. However, when senders were synchronized with a transmission delay $|\delta| < 10$ µs, *the PRR was over* 99 %.

We confirm these findings running experiments on channel 5[4] using the default BASE configuration described in § 3, which employs a standardized PSR of 64 (a PSR of 128 is vendor-specific). While the sender in *link 1* transmits frames 2 ms after receiving the synchronization beacon, the sender in *link 2* introduces an extra transmission delay δ between ±60 µs.

[3]We consider concurrent transmissions of packets with different payload, whose reception is harder than that of packets with the same payload [62].

[4]Unlike channel 4, channel 5 is widely available in off-the-shelf UWB radios and recommended for worldwide regulatory acceptance [60] (see Tab. 1).

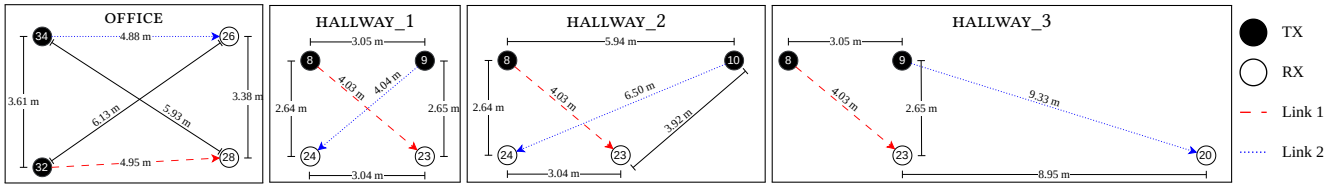

Figure 3: Sketch of the four measurement scenarios used in § 4 – § 6. The actual placement of the devices within the testbed can be inspected by matching the device IDs to those depicted in Fig. 2. Experiments in the OFFICE use device 36 as initiator, whereas experiments in the HALLWAY use device 35 as initiator.

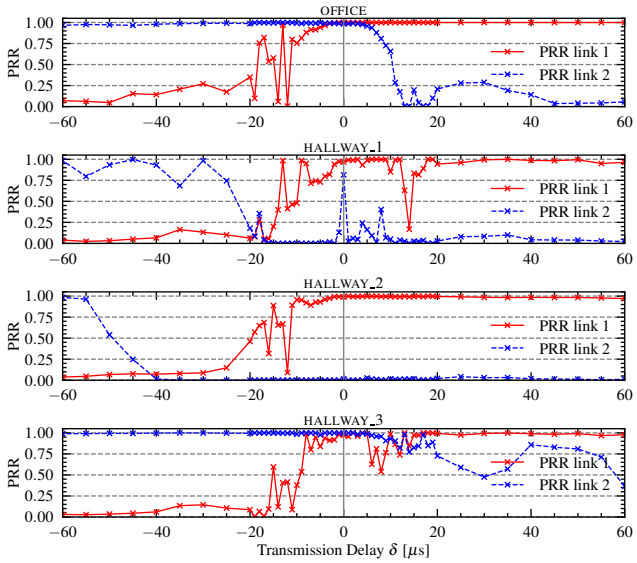

Figure 4: PRR of two concurrent transmissions in four different scenarios using the BASE configuration.

Fig. 4 shows the PRR of the two links in the four different scenarios as a function of δ. Focusing on the OFFICE scenario first, one can observe that the PRR of the link in which the sender initiates the transmission earlier[5] is close to 100 %, whereas the PRR in the other link is close to zero (i.e., the earlier transmission overshadows the later one). However, for $|\delta|$<10 µs, the average PRR for both links is above 90 %, which indicates the positive impact of synchronization and confirms the observations in [62]. A similar trend can be observed in HALLWAY_3. Whilst also here the earlier transmission overshadows the later one, due to the considerable distance between the *link 2* receiver and the *link 1* transmitter, the PRR of *link 2* never falls below 36 % for any δ. Also in HALLWAY_3, the average PRR of both links is highest (≥90 %) for a tight synchronization ($|\delta|$<5 µs).

A different pattern can be seen in HALLWAY_1 and HALLWAY_2, where the PRR of *link 2* deteriorates at a lower δ compared to the previous scenarios. Specifically, a transmission on *link 2* has to occur at least 20 µs and 40 µs before that of *link 1* in HALLWAY_1 and HALLWAY_2, respectively, to have a chance of being received.

Fig. 5 shows the average PRR across the two links as a function of $|\delta|$ in all four considered scenarios. As observed in Fig. 4, whilst HALLWAY_3 shows a comparable trend to OFFICE (with an average PRR across both links close to 100 % for low values of $|\delta|$,

[5]When $\delta < 0$, the sender of *link 2* initiates the transmission earlier; when $\delta = 0$, the transmissions in the two links occur at the exact same time; when $\delta > 0$, the sender of *link 1* initiates the transmission earlier.

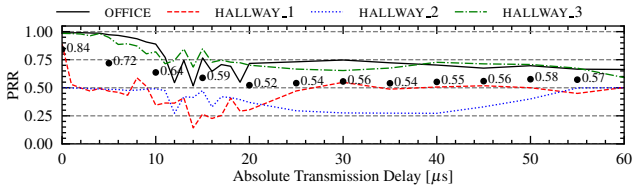

Figure 5: Average PRR across *link 1* and *link 2* as a function of $|\delta|$ in the four scenarios (BASE configuration). The numbers indicate the mean PRR across all scenarios.

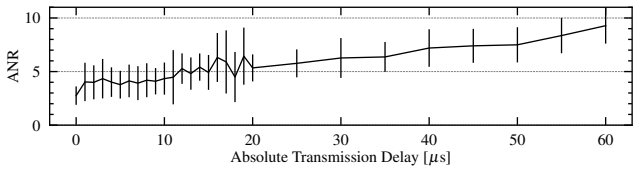

Figure 6: Average ANR across the four different scenarios as a function of the absolute transmission delay.

and close to 50 % when synchronization is loose[6]), the performance in HALLWAY_1 and HALLWAY_2 is considerably worse. Specifically, in HALLWAY_1 the average PRR peaks at 85.29 % for $|\delta| \leq 1$ µs and quickly drops to the 50 % mark for higher values of $|\delta|$. In HALLWAY_2, instead, a tight synchronization across concurrent transmitters alone *does not help* in allowing reception of packets in *link 2*: the PRR is hence always around 50 % regardless of δ, hinting that only *link 1* operates correctly.

These results can be explained by inspecting the physical location of the device pairs shown in Fig. 3. In OFFICE, for each link (i.e., device pair), the TX is closer to the RX than the transmitter in the other link. In HALLWAY_3, this is the case for *link 2* (i.e., node 9 is closer to node 20 than node 8). In HALLWAY_1 and HALLWAY_2, instead, the transmitter of the other link is always closer to RX: in HALLWAY_1, for example, node 8 is closer to node 24 than node 9 (and node 9 is closer to node 23 than node 8). In HALLWAY_2, node 8 is significantly closer to node 24 than node 10, which explains why *link 2* has a PRR consistently close to zero (see Fig. 8).

We also investigate the impact of a tight synchronization across concurrent transmitters on the ANR. Fig. 6 shows that the signal quality of the received CIR increases linearly with $|\delta|$. In fact, when $|\delta|$=0, the concurrently-transmitted preambles overlap entirely (ANR=2.76). When $|\delta|$=60 µs, the concurrently-transmitted preambles only overlap in the air for 4 µs, resulting in a three times higher ANR of 9.28.

[6]Note that, when the average PRR converges towards 50 % for high values of δ, only the link where the sender initiates the transmission earlier correctly receives packets.

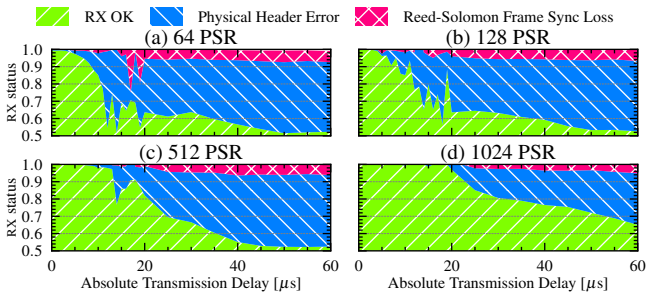

Figure 7: Reception status in OFFICE for different PSR.

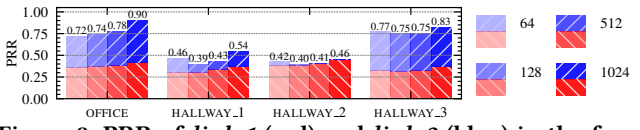

Figure 8: PRR of *link 1* (red) and *link 2* (blue) in the four scenarios for different PSR[7].

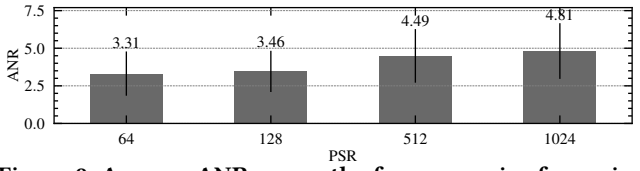

Figure 9: Average ANR across the four scenarios for an increasing number of PSR when using a fixed $|\delta| \leq 1\,\mu s$.

Takeaways. When multiple UWB devices communicate concurrently over different complex channels, earlier transmissions have a higher chance of being received. Often (but not always), the chances of receiving also the later transmissions increase when the relative delay between transmissions is low (the smaller the better). Based on these findings, *we propose an enhanced configuration named* SYNC, in which concurrent transmitters maintain a synchronization within $\pm 1\,\mu s$. The use of SYNC (which is equivalent to the BASE configuration with $|\delta| \leq 1\,\mu s$) allows to obtain an average PRR across the 4 considered scenarios of 83 %, as shown in Fig. 5.

5 OPTIMIZATION OF PHY SETTINGS

Building upon our experiments in § 4, we first shed light on the cause for packet loss (§ 5.1), identifying the incorrect detection of the SFD within the SHR as one of the main sources of problems. We then investigate the impact of different SHR settings, including *preamble lengths* (§ 5.2), *preamble codes* (§ 5.3), and *SFD sequences* (§ 5.4) on the reliability of concurrent transmissions over different complex channels.

5.1 Understanding Packet Loss

We inspect the receiver status information of RX nodes to identify the root cause of packet loss. Fig. 7(a) breaks down the correct and incorrect receptions in OFFICE as a function of $|\delta|$. Most errors when $|\delta| > 10$ occur while decoding the PHR, whereas only a small fraction of errors are payload-related (i.e., are Reed-Solomon decoding errors).

The most obvious reason for a physical header error (PHE) is the presence of an interference signal during the reception of the PHR. However, the transmission of the PHR commonly takes only 19 µs when using the nominal data rate of 850 kbit/s, and Fig. 7(a) hints that PHEs are dominant even for $|\delta| > 19\,\mu s$, leading to a different explanation. Earlier work has shown that Qorvo's DW1000 and DW3000 radios may identify arbitrary radio signals (e.g., Wi-Fi 6E traffic) as preamble symbols or as SFD [53]. We hence infer that the concurrent transmissions on another complex channel may trigger an erroneous SFD detection, which causes the radio to attempt decoding the PHR before it was sent.

Increasing the robustness of the SHR and the probability to correctly detect the SFD should hence improve the reliability of concurrent transmissions over different complex channels.

5.2 Impact of the Preamble Length

The length of the preamble plays a crucial role w.r.t. the robustness of the SHR and of a UWB frame in general [29]: while short preambles increase energy efficiency, long preambles improve reliability. To examine the impact of the preamble length, we repeat the experiments shown in § 4 by varying the number of PSR between 64 and 1024 symbols.

Figs. 7(b–d) illustrate our results, revealing that longer preambles increase the PRR and *relax the necessary synchronization across concurrent transmitters to reliably communicate*. For example, in OFFICE, to achieve a PRR of 90 %, one requires $|\delta| < 9\,\mu s$ when using 64 PSR, whereas $|\delta| < 12$, 14, and 20 µs is sufficient when using 128, 512, and 1024 PSR, respectively.

Notably, the number of Reed-Solomon errors does not increase with δ, which supports our previous assumption. Fig. 8 shows the benefits introduced by a higher number of PSR in the four scenarios. In OFFICE, the PRR[7] grows from 71.84 % to 89.83 % when increasing the number of PSR from 64 to 1024. In HALLWAY_1, HALLWAY_2, and HALLWAY_3, the increase in PSR leads to a less pronounced (but still significant) improvement in PRR of 7.8, 3.3, and 5.7%, respectively[8].

Fig. 9 shows the signal quality in terms of ANR for increasing preamble lengths, averaged over the four different scenarios. Note that, to avoid mixing the impact of the transmission delay on the results, the figure only shows the case in which $|\delta| \leq 1\,\mu s$ (SYNC). The ANR increases by 45% when increasing the number of PSR from 64 (ANR=3.31) to 1024 (ANR=4.81).

Takeaways. Increasing the number of PSR improves the signal quality and allows to increase the reliability of concurrent communications (i.e., one can achieve a comparable PRR than when using less PSR with more relaxed synchronization constraints). The use of a higher PSR comes with a higher energy expenditure, which will be quantified in § 7.

5.3 Impact of the Preamble Code

All previous experiments have been performed with preamble codes 9 (for *link 1*) and 10 (for *link 2*). Since 16 preamble codes are defined

[7]Note that the PRR is averaged for different values of δ (i.e., across the entire ±60 interval captured in our experiments, as described in § 3).

[8]Note that a slight drop in PRR is visible when using 128 instead of 64 PSR. This is likely because we have performed measurements with 64 PSR using the optimized receiver configuration (i.e., the `dwt_configurefor64plen()` function), as suggested by the Qorvo DW1000's API guide [15].

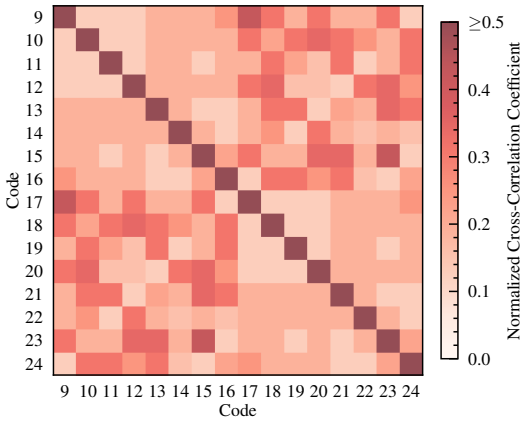

Figure 10: Correlation matrix for the 16 preamble codes used with 64 MHz PRF.

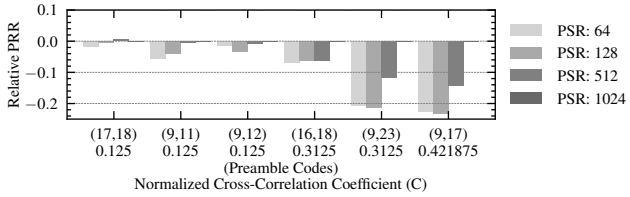

Figure 11: PRR of different preamble code combinations (i, j) in OFFICE relative to the use of $(9, 10)$[7].

by the standard for a PRF of 64 MHz (numbered from 9 to 24), we examine if and to which extent their choice affects the performance of concurrent transmissions.

As discussed in § 2.2, although preamble codes were designed to have an ideal auto-correlation property, some correlation among different codes remains [18]. We quantify the latter by defining the normalized cross-correlation coefficient C of two codes (i, j)[9], and illustrate C for all code combinations in Fig. 10. Preamble codes 9–12 and 17–20 share a low cross-correlation (0.125) among each other (lighter color).

To investigate the impact of an increasing cross-correlation coefficient, we repeat the previous experiments with other preamble code combinations in the OFFICE scenario. Fig. 11 shows the PRR obtained with a given PSR and preamble code combination relative to the PRR obtained with the same PSR when using preamble codes 9 and 10. We observe similar PRR values (at most a 5.4 % deviation) when using preamble code combinations having a low C such as (17,18), (9,11), and (9,12), whereas we notice a significant decrease (by up to 23.11 %) when using preamble code combinations having a high C. When using 1024 PSR, there is no difference in the observed PRR, *regardless of the chosen preamble code combination and its cross-correlation.* This hints that the use of a long preamble allows to neutralize the negative impact caused by the use of preamble code combinations with high C. In terms of signal quality, the ANR does not show a significant relation to C.

[9]Let $cor(i, j)$ be the correlation between two codes i and j. As suggested in [34], we define their normalized cross-correlation coefficient $C(i, j) = max(|cor(i, j)|)/\sqrt{max(|cor(i, i)|) * max(|cor(j, j)|)}$.

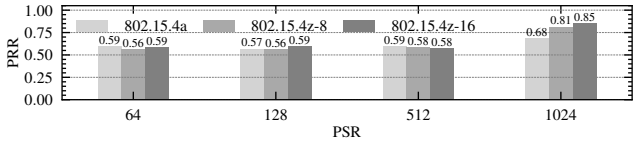

Figure 12: Average PRR across the four scenarios as a function of the number of PSR and used SFD sequence[7].

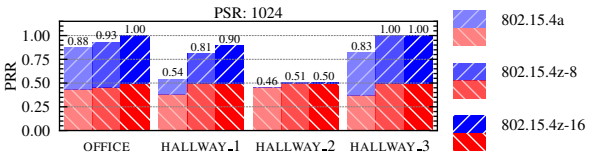

Figure 13: Mean PRR of *link 1* (red) and *link 2* (blue) for 1024 PSR and different SFD sequences in each scenario[7].

Takeaways. Selecting preamble codes having low cross-correlation improves reliability, especially for transmissions with short preambles. Using 1024 PSR yields the same PRR regardless of the employed preamble code combination.

5.4 Impact of the Start-of-Frame Delimiter

With the introduction of the IEEE 802.15.4z amendment [33], new SFD sequences have been introduced. Because of their extended length (up to 32 symbols) and the absence of zeros, these new SFD sequences are supposedly more resilient, making them a promising choice to enhance the reliability of the SFD detection. Although the DW1000 radio used in our experiments was introduced before the IEEE 802.15.4z amendment (and hence does not implement these new sequences), it allows to use *user-defined spreading sequences* [18] up to a length of 16 symbols. We use this feature to enable the new IEEE 802.15.4z SFDs on the DW1000, and verify that a radio implementing the new SFD sequences (the Qorvo DWM3001 CDK) can correctly receive the transmitted frames.

Fig. 12 shows the average PRR of the two links across the four examined scenarios as a function of the employed SFD sequences and number of PSR. Using the new SFD sequences is particularly beneficial when using large preambles (i.e., with 1024 PSR), where the average PRR increases from 68.12 % to 84.98 %. For shorter preambles, we observe a slight decline in PRR up to 3% when using the new SFD sequences.

Fig. 13 shows the average PRR sustained when using the three SFD sequences in combination with a PSR of 1024 for each scenario. The use of the longer SFD allows to reach a perfect reliability in OFFICE and HALLWAY_3, increases the PRR from 54.23 % to 89.51 % in HALLWAY_1, and allows *link 1* to sustain a perfect reception in HALLWAY_2 (although *link 2* is still unusable). In terms of signal quality, the used SFD sequence has a negligible impact on the ANR: in fact, the CIR estimation is based on the preamble sequence only.

Takeaways. Using the SFD sequences from the IEEE 802.15.4z amendment in combination with a high number of PSR allows to effectively improve reliability.

Based on these findings, *we propose an enhanced configuration optimizing the radios' PHY settings, named* OPT (Tab. 3), in which we use 1024 PSR in combination with the length-16 IEEE 802.15.4z SFD sequence. As shown in Fig. 13, OPT sustains an average PRR of 85 %

Table 3: PHY settings used in the OPT configuration.

Preamble symbol repetitions (PSR)	1024
Pulse repetition frequency (PRF)	64 MHz
Data Rate	6.8 Mbps
SFD sequence	IEEE 802.15.4z (16 symbols)
Preamble code	9 and 10

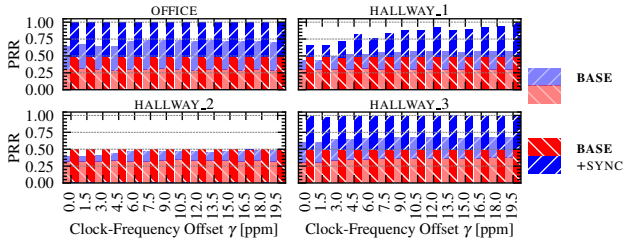

Figure 14: Mean PRR of *link 1* (red) and *link 2* (blue) in each scenario when using BASE as a function of γ.

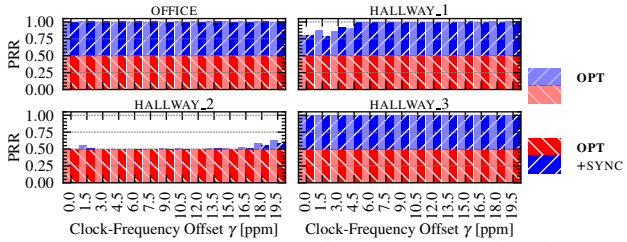

Figure 15: Mean PRR of *link 1* (red) and *link 2* (blue) in each scenario when using OPT as a function of γ.

across the four scenarios compared to the 59 % of the BASE configuration. Thus, while using OPT increases airtime and hence decreases energy efficiency compared to BASE, it allows for coexistence among different uncooperative UWB-based systems or devices, especially in the absence of clear-channel assessment capabilities that UWB unfortunately lacks.

6 UTILIZING CLOCK DETUNING

A few recent works have emphasized the impact of the CFO on the reliability of concurrent transmissions [5, 39, 41]. We hence artificially vary the CFO between device pairs in each scenario depicted in Fig. 3, so to investigate the impact of the CFO on the separation of UWB complex channels.

To this end, as discussed in § 3, upon the reception of the initiator's beacon we let *link 1*'s TX and RX use the radio's trimming feature to set a CFO of 0 with respect to the initiator. However, we now configure *link 2*'s TX and RX to match a CFO γ, which we vary between 0 and 19.5 ppm in steps of 1.5 ppm[1]. We then send 2000 packets per measurement using a randomized transmission delay $\delta \in [-60, +60]$ μs in the BASE configuration and $\delta \in [-1, +1]$ μs in SYNC (instead of enforcing specific values at fixed steps) to better generalize our results. We also run an OPT configuration resembling BASE, but with optimized PHY settings, as detailed in § 5.4 and summarized in Tab. 3.

Impact on reliability. Figs. 14 and 15 show that larger CFOs across concurrent transmitters (i.e., larger values of γ) help increasing the PRR, (i) both in presence and in absence of a tight synchronization

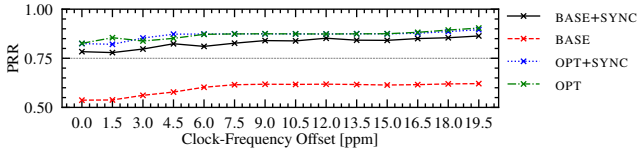

Figure 16: Reliability as a function of an increasing γ averaged across the four considered scenarios.

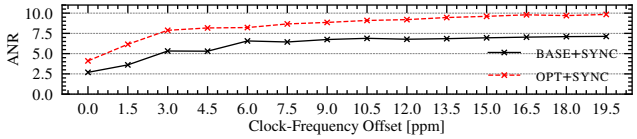

Figure 17: ANR as a function of an increasing CFO averaged over the four investigated scenarios.

(SYNC) across concurrent transmitters, as well as (ii) with or without optimized PHY settings (OPT).

In OFFICE and HALLWAY_3, the use of a tight synchronization and/or of optimized PHY settings already allows to sustain a PRR of 100% on both links regardless of γ. When using BASE alone, instead, the PRR in these two scenarios grows by 7% and 8%, respectively, when increasing γ from 0 to 19.5.

In HALLWAY_1, the use of SYNC or OPT alone in absence of CFO (i.e., when $\gamma = 0$) is not sufficient to sustain a PRR close to 100% on both *link 1* and *link 2*. However, introducing a CFO allows to obtain a PRR $\approx$ 100% when using BASE + SYNC with $\gamma = 19.5$, and when using OPT (+SYNC) with $\gamma \geq 4.5$.

In HALLWAY_2, regardless of γ, the use of SYNC or OPT allows a perfect reception over *link 1* (red), which is not possible with the BASE configuration alone. When using OPT (+SYNC) with $\gamma > 15$ ppm, also a few packets over *link 2* (blue) start to be received: the combined PRR grows from 50 % (i.e., only *link 1* operational) up to 61.95 % (i.e., a few packets within *link 2* can now also be received). While this PRR is still insufficient to allow a proper communication on *link 2*, we will show in § 8 that aggressively detuning the CFO further by fine-tuning the operating parameter set (OPS) of the radio allows to boost the PRR of *link 2* well above 90%.

Fig. 16 shows the PRR averaged across all scenarios as a function of γ, and confirms that introducing a CFO across concurrent transmitters helps increasing reliability for all explored configurations (BASE, BASE + SYNC, OPT, OPT + SYNC). Already when introducing a CFO of 4.5 ppm, we observe an average improvement in PRR across all scenarios by 4.13 % with BASE and 2.54 % with OPT. An interesting observation that stems from Fig. 16 is that the PRR obtained when using OPT + SYNC is on par with the PRR obtained using OPT alone. This hints that the use of OPT allows to forego the need for a tight synchronization, as further elaborated in § 7.

Impact on signal quality. Fig. 17 shows that introducing a CFO also increases the signal quality for both the BASE and OPT configuration. In fact, the ANR improves from 2.69 to 7.13 when introducing a CFO of 19.5 ppm using BASE (from 4.10 to 9.84 when using OPT), and the improvement is already quite significant for small offsets (e.g., 4.5 ppm). Note that, as in Fig. 9, we consider the case in which $|\delta| \leq 1$ µs (SYNC) to avoid mixing the impact of the transmission delay on the results. Fig. 18 visualizes the improvements in signal quality by showing 100 CIR estimates recorded on node 36 in the

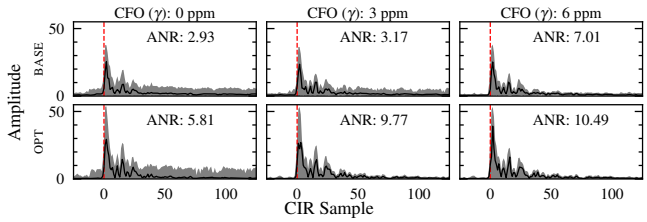

Figure 18: Excerpts of CIR estimates recorded in OFFICE using BASE and OPT with increasing CFOs. The CIRs are aligned to the detected first path (red dashed line).

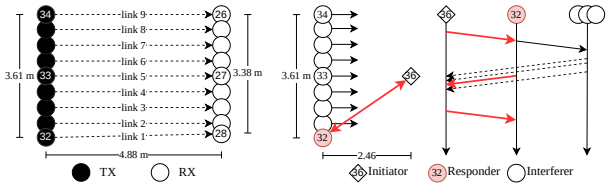

(a) Reliability (b) Ranging performance

Figure 19: Setup to evaluate the reliability and ranging performance of multiple concurrent transmissions.

OFFICE scenario with different CFOs using both the BASE and OPT configurations (with the black and grey line indicating the median and maximum measured amplitude value for each sample, respectively). Visibly, when increasing γ, the noise in the CIR reduces, which ultimately leads to a higher ANR.

We conjecture the improvement in signal quality when introducing a CFO is due to a phase shift during the reception of the SHR. Indeed, the impact of the CFO on the cross-correlation of different preamble codes can be modelled as described by Liu et al. [34]. In future work, we will investigate this aspect using signal-level simulation (see § 8).

Takeaways. Detuning the clock (i.e., introducing a CFO across concurrent transmitters) can complement the use of a tight synchronization and optimized PHY settings to effectively increase the reliability and signal quality of concurrent communications. Introducing small offsets (e.g., 4.5 ppm) is already quite effective, as visible in Figs. 16 and 17. Based on these findings, we propose an enhanced configuration introducing a CFO of 5 ppm between devices operating on different complex channels, named DETUNE, as further elaborated in § 7. Utilizing DETUNE on top of the BASE configuration across the four investigated scenarios improves the PRR by 6.57 % and the ANR by 47% (i.e., from 4.30 to 6.32).

7 PUTTING THINGS TOGETHER

§ 4–6 have shown the effectiveness of three tuning levers (SYNC, OPT, and DETUNE) to increase the performance of concurrent UWB communications. We consider next *all possible permutations* of SYNC, OPT, and DETUNE, evaluating their performance with up to *nine concurrent transmissions* in terms of communication reliability (§ 7.1) and ranging performance (§ 7.2). We then discuss the applicability of these tuning levers in real-world use cases, their management overhead, channel occupancy, and energy efficiency (§ 7.3).

7.1 Reliability of Multiple Transmissions

To investigate the effectiveness of the proposed tuning levers (SYNC, OPT, DETUNE) and their combinations in increasing the reliability of communications when scaling up the number of concurrent transmitters, we focus on a scenario in which up to 9 pairs of devices transmit data concurrently.

Experimental setup. As shown in Fig. 19(a), we reuse a portion of the nodes installed in the testbed (see Fig. 2) to form nine TX–RX devices pairs (*links 1–9*) using preamble codes 9–17 (i.e., operating on nine different complex channels). As for § 3–6, we send 2000 frames with randomized payload, and vary the synchronization

Table 4: Configurations tested in § 7.

Configuration	PHY	γ	δ
BASE	PSR: 64 SFD: 802.15.4a	±60 µs	0 ppm
BASE +DETUNE			5 ppm
BASE +SYNC		±1 µs	0 ppm
BASE +SYNC +DETUNE			5 ppm
OPT	PSR: 1024 SFD: 802.15.z-16	±60 µs	0 ppm
OPT +DETUNE			5 ppm
OPT +SYNC		±1 µs	0 ppm
OPT +SYNC +DETUNE			5 ppm

across concurrent transmitters by applying a random transmission delay $\gamma \in [-60, +60]$ μs to resemble uncoordinated arbitrary traffic.

We use a baseline configuration (BASE) using the PHY settings listed in Tab. 2. OPT uses 1024 PSR in combination with the length-16 IEEE 802.15.4z SFD sequence (see § 5.4). SYNC employs a random transmission delay within ±1 µs (see § 4).

The use of DETUNE demands a separation of at least γ=5 ppm among complex channels (see § 6): considering the ±20 ppm trim range of the DW1000 radio, this allows us to use up to nine complex channels[10]. We hence let each link's TX and RX devices calculate their relative CFO to an initiator (INIT node 36) periodically broadcasting beacons and adjust their clock frequency as to match an alternating CFO[11]. Tab. 4 summarizes the configurations tested in our experiments.

Results. Fig. 20 shows the PRR as a function of the number of complex channels used simultaneously (i.e., 1 complex channel means that only *link 1* is active, 2 complex channels means that *link 1* and *link 2* are concurrently active, etc.).

The reliability of BASE drops with the number of concurrent transmissions (with a PRR of only 22 % across 9 links). Whilst BASE+DETUNE does not help improving reliability, the use of BASE+SYNC is quite effective (we observe a PRR of 91.33 % and 75.75 % for seven and nine concurrent transmissions, respectively). When using DETUNE in combination with BASE and SYNC, we observe an even higher PRR (94.73 % and 87.43 % for seven and nine concurrent transmissions).

The use of optimized PHY settings leads to the best results: OPT alone allows to sustain a PRR of 94.03 % for nine concurrent transmissions (outperforming the PRR obtained with BASE+SYNC+DETUNE).

[10]Note that 9 is a limit dictated by the trim range of the DW1000 radio and by the use of γ=5 ppm. Decreasing γ and using a radio supporting a higher trim range would allow to support a higher number of complex channels.
[11]We set *link 1*: 0 ppm, *link 2*: 5 ppm, *link 3*: -5 ppm, *link 4*: 10 ppm, *link 5*: -10 ppm, *link 6*: 15 ppm, *link 7*: -15 ppm, *link 8*: 20 ppm, *link 9*: -20 ppm.

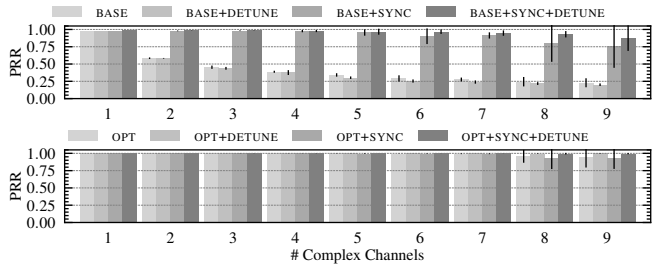

Figure 20: Reliability (PRR) of different configurations for an increasing amount of complex channels.

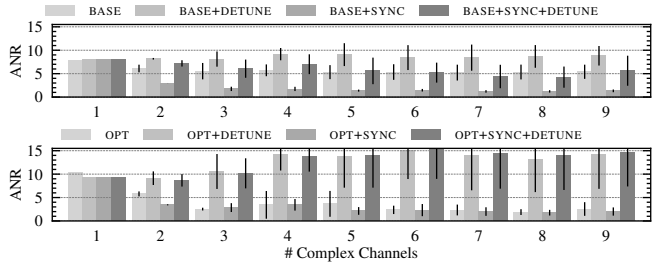

Figure 21: Signal quality (ANR) of different configurations for an increasing amount of complex channels.

The highest reliability is observed with OPT+DETUNE, which allows to sustain a near-perfect reception (a PRR of 99.81 %) for nine concurrent transmissions. In line with what observed in § 6, the use of SYNC in addition to OPT does not improve reliability further. Notably, these results show little deviation among the different concurrent links, indicating a low device-specific impact on the results.

Fig. 21 shows the signal quality as a function of the number of complex channels used for different combinations of tuning levers. In general, the ANR decreases with the number of complex channels when using BASE and OPT alone. The use of SYNC on top, as shown in § 4 (Fig. 6) reduces the ANR further. Importantly, in line with the results shown in § 6, the use of DETUNE on top of BASE and OPT allows to boost the signal quality. When using OPT+DETUNE(+SYNC), the ANR becomes even higher when using several complex channels simultaneously. The reason can be found in the number of preamble symbols used during the preamble accumulation in the radio diagnostics. Notably, the DW1000 radio does not accumulate all transmitted preamble symbols during the synchronization, but stops after exceeding a saturation threshold. With only one complex channel, the receiver accumulates on average only 271 out of 1024 preamble symbols. With 9 concurrently-used complex channels, 571 out of 1024 preamble symbols are considered, which reduces the noise at the receiver when using DETUNE.

7.2 Impact on Ranging Performance

We study next whether the proposed tuning levers affect the accuracy and precision of UWB ranging measurements.

Experimental setup. We use the setup shown in Fig. 19(b) to perform 2000 double-sided two-way ranging measurements between an initiator (node 36) and a responder (node 32) in the presence of up to 8 additional nodes communicating on other complex channels

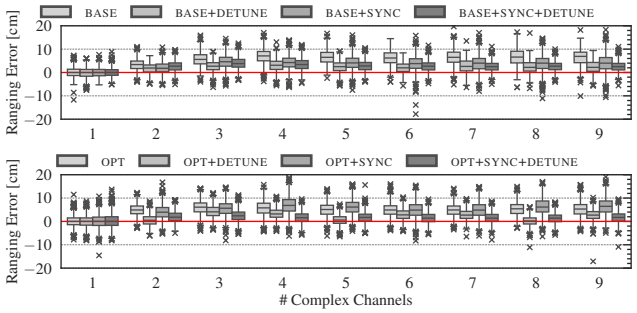

Figure 22: Ranging performance of different configurations for an increasing amount of complex channels.

(i.e., practically interfering with the second message sent within the ranging process between the responder and the initiator).

Results. Fig. 22 shows the accuracy and precision of the obtained ranging measurements as a function of the number of simultaneously-active complex channels. Both ranging accuracy and precision decrease when several complex channels are operating concurrently. Specifically, the median of the introduced ranging offset in the presence of more than four concurrent transmitters increases by 69 mm and 52 mm when using BASE and OPT alone, respectively. In line with the trends shown by the ANR, the use of SYNC does not improve ranging performance, whereas the use of DETUNE allows to decrease the ranging offset median to 22 mm (BASE+DETUNE), 27 mm (OPT+DETUNE), or 17 mm (OPT+SYNC+DETUNE).

Therefore, the introduced tuning levers not only increase the reliability of communications compared to BASE (§ 7.1): they also reduce the ranging offset caused by concurrent transmissions in other complex channels. That is, the proposed methods can be used to improve and scale up UWB systems while retaining the ability to perform cm-accurate ranging.

7.3 Applicability of the Proposed Methods

We have shown in § 7.1 and 7.2 how SYNC, OPT, and DETUNE (and permutations thereof), can improve reliability and ranging performance for up to 9 concurrent transmitters on the same frequency[10]. Yet, real-world wireless systems often need to satisfy strict requirements, which may require compromises w.r.t. the use of these techniques. We hence highlight next each technique's benefits and costs.

SYNC. In order to use SYNC in real-world applications, devices must adhere to a common time source and maintain a transmission delay $|\delta| \leq 1\,\mu s$. Establishing synchronization in low-power wireless networks has been well-investigated [59], and large-scale time-division multiple access (TDMA) based media access (MAC) protocols such as TSCH are capable of establishing sub-μs synchronization [21] even over multiple hops[12]. Such concepts have already been ported to and proven with UWB [11]. Moreover, the excellent timing resolution of UWB flooding-based approaches has been shown to provide ns-accurate synchronization [41], and can be readily leveraged.

However, SYNC has two main drawbacks. Firstly, maintaining synchronization may increase the communication overhead as well as

[12]Note that, to apply SYNC, only a synchronization within the direct neighbourhood is required: there is no need for an expensive network-wide synchronization.

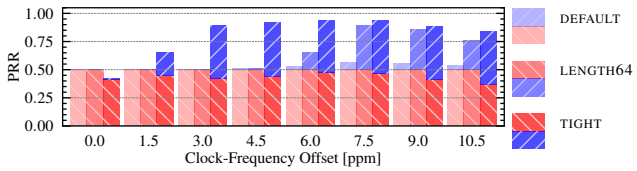

Figure 23: PRR for the OPT parameter set with different OPS, for increasing CFOs in the HALLWAY_2 secenario.

the overall complexity [59], imposing an additional energy cost[13]. Secondly, one cannot synchronize unmanaged devices, such as those present in a co-located but independently-deployed UWB systems from a different vendor.

SYNC is hence suitable for systems where synchronization is inherent within the underlying protocols, such as systems using a TDMA- or flooding-based protocol (e.g., IEEE 802.15.4 TSCH-based networks used in industrial deployments), but does not provide a solution for the coexistence with co-located systems from different vendors.

OPT. Due to the lack of clear-channel assessment capabilities of UWB radios – that could prevent colliding transmissions and would allow the consecutive transmission using the BASE configuration – optimizing UWB PHY settings represents the most effective way to increase reliability in the presence of interference from other UWB devices. This is also applicable when faced with external interference from co-located UWB networks deployed by other vendors. Unlike SYNC, configuring the PHY settings is a one-time or on-demand activity, which does not incur a continuous management overhead. However, the large improvement in reliability brought by OPT comes at the cost of longer packet airtime, which increases latencies and reduces the system's throughput and energy efficiency. The BASE configuration employs a short preamble and SFD: sending a 120-byte frame hence takes 236.35 µs (assuming a data rate of 6.8 Mbit/s). Conversely, the OPT configuration takes 1221.27 µs for the same amount of data (i.e., 4.6x more). When using a DW1000 radio, this means an energy consumption of 41.76 µJ (TX) and 87.94 µJ (RX) with BASE, and of 258.96 µJ (TX) and 443.40 µJ (RX) with OPT [17].

OPT is hence most suitable when there is a need to coexist with other nearby UWB systems, but only when energy consumption is not an overriding concern (e.g., in systems involving UWB-enabled smartphones, where the energy consumed by the UWB radio is a tiny fraction of the overall energy usage).

DETUNE. As shown in the previous sections, not only does CFO detuning help to improve reliability and ranging performance, but it presents the opportunity to 'piggyback' on mechanisms already inherent within the IEEE 802.15.4 standard. By introducing additional diversity through the CFO, detuning supports scalability and minimizes internal interference within the UWB system, but introduces complexity in the form of a scheduling problem, as transmitting nodes must ensure orthogonality. However, this could also align with current approaches in time-synchronized wireless sensor networks. For example, adopting the approach of IEEE 802.15.4 TSCH-based systems, one can extend the definition of a complex channel from `(freq, pc)` to `(freq, pc, cfo)`, with `freq` being the frequency channel, and `pc` the preamble code. Importantly, detuning comes at *zero cost* w.r.t. energy, channel occupancy, and throughput; furthermore, extending signalling mechanisms that are already present within the standard would incur little or no additional overhead.

DETUNE can hence scale up UWB-based systems in single-vendor scenarios, where devices are managed. While the added CFO diversity does not address the issue of external interference from unmanaged co-located networks, there is the opportunity to explore how to improve poorly-performing channels (e.g., through the random selection of a new CFO, or by identifying the interference and adjusting the CFO accordingly). Such approaches would also combat external interference.

Recommendations. In light of the aforementioned benefits and drawbacks associated with these three methods, and considering results presented in § 4–6 as well as § 7.1–7.2 where we explore different permutations thereof, we can hence broadly recommend the following for practitioners wishing to employ these techniques within their systems: (i) *in low-energy systems, BASE+SYNC+DETUNE provides the best performance; (ii) in scenarios where energy requirements are not so strict, then OPT+DETUNE should be used.*

8 DISCUSSION AND FUTURE WORK

Device-specific receiver optimizations. In this paper, we derived methods that can be implemented using any standard-compliant radio. In principle, one could also leverage vendor-specific extensions to further improve performance. For example, one could use the three operating parameter sets (OPS) offered by the DW1000 radio (DEFAULT, LENGTH64, and TIGHT [18])[14] to improve the effectiveness of DETUNE. Fig. 23 shows the mean PRR of *link 1* (red) and *link 2* (blue) in HALLWAY_2 when using OPT as a function of different CFOs. As seen in § 3–6, HALLWAY_2 is particularly challenging due to the relative placement of the nodes (causing a high signal-to-interference ratio), and none of the proposed tuning levers (OPT, SYNC, DETUNE) seemingly allows to receive the packets sent in *link 2* (see Fig. 15). Interestingly, using DETUNE in conjunction with specific OPS allows reliably receiving these packets. In fact, when using the TIGHT OPS with a CFO of 6 ppm, we sustain a 93.86% PRR. This hints that the separation between complex channels can be increased by configuring a tighter CFO range via the OPS.

Features of next-generation UWB transceivers. While Qorvo's DW1000 radio has been the foundation for most UWB research in recent years, with the introduction of the IEEE 802.15.4z amendment a new generation of UWB radios has emerged (such as the Qorvo DW3000) with additional features and improvements. Studying whether our findings apply also to these radios is hence a very interesting avenue for future work. Indeed, we expect that these radios will further improve the performance of the tuning levers proposed in this work. For example, besides the support of channel 9, the Qorvo DW3000 offers more fine-grained control of the clock trim and finer tuning of the preamble length: these should allow,

[13] Even though the energy overhead of synchronization can be optimized, e.g., by using adaptive synchronization [8, 57], the tradeoff between necessary synchronization accuracy and energy consumption imposes significant challenges, primarily when relying on an energy-efficient real-time clock instead of the high-precision radio-clock found on UWB radios.

[14] While the user manual recommends using the DEFAULT setting [18], it states that each OPS allows to limit the range of the feasible CFO between transmitter and receiver (DEFAULT: ±40 ppm, LENGTH64: ±15 ppm, TIGHT ±1 ppm) by restricting the pull-in range of the receiver's phase-locked loop.

respectively, to increase the accuracy and effectiveness of DETUNE and to further improve the energy efficiency of OPT.

Beyond empirical evidence. Most of the insights presented in this work are of empirical nature, and hence inherently linked to the studied scenarios (cf. Fig. 3 and Fig. 19). In the future, to better generalize our findings, we plan to carry out similar investigations in a controllable, wired experimental setup.

Better understanding of the role of the CFO. In § 6 we have argued that the underlying reason for the signal quality improvement obtained when introducing a CFO is likely a phase shift during the reception of the SHR. We plan to validate this conjecture in the near future using a full signal-level simulation and an in-depth analysis on a conducted measurement setup.

Use of secure ranging. New-generation UWB radios compliant to IEEE 802.15.4z enable a secure estimation of the time-of-arrival of the signal by introducing a scrambled timestamp sequence (STS) within the transmitted frames [58]. Like the preamble acquisition of the SHR, the STS correlates against a known sequence. However, STS symbols do not follow the Ipatov construction and might share a high cross-correlation with other symbols on the air. Future work should hence investigate whether performance drops when multiple frames embedding an STS are sent concurrently. Should this be the case, the ability to fine-tune the STS length could be used (and added to OPT) to tackle the issue.

Extension of UWB MAC protocols. Our findings can be used to enrich many of the UWB MAC protocols proposed in the literature. For example, TSCH could be extended by including complex channels as additional component within the traditional TDMA schedule. When using the BASE configuration to prioritize energy, SYNC would be provided for free through the existing TSCH sub-μs synchronization mechanisms [21]. One could also adapt the TSCH schedule to accommodate longer slot times (e.g., through dynamic slots [4]) and prioritize reliability using OPT. Alternatively, random access protocols for UWB [3] could make use of the OPT configuration to improve channel separation.

9 RELATED WORK

Following the growing popularity of UWB technology and its increasing use to design location-aware IoT applications, a large number of research studies have focused on improving the reliability and performance of UWB-based systems.

Fine-tuning UWB PHY settings. Several works have studied the impact of different PHY settings on the reliability of UWB communication [2, 29, 62] and ranging [26, 44], but without focusing on concurrent transmissions over different complex channels. In this work, we have been – to the best of our knowledge – the first to analyze the impact of several UWB PHY settings on the reliability of communications as well as on the accuracy and precision of ranging in the presence of multiple concurrent transmissions. Ansaripour et al. [3] have previously shown using the DW3000 radio that a low preamble acquisition chunk (PAC) size – a parameter that impacts the number of preamble symbols that are correlated in parallel – could reduce the interference across complex channels. However, a low PAC size is typically recommended for short preambles only [18]. In our experiments, we have used exclusively the vendor's recommendation for the PAC size, which scales along with the preamble length [18].

Concurrent UWB transmissions. Concurrent transmissions have gained popularity in the low-power wireless community within the last decade [9, 65]. This holds true also for UWB systems since solutions based on the Glossy work [23] have been ported to UWB [41], sparking follow-up research enabling highly-reliable and energy-efficient UWB communication [37, 39, 56, 61]. However, this body of work leverages concurrent transmissions to disseminate *a single message* and to provide synchronization over a network. In contrast, our work aims to enable the transmissions of *multiple concurrent messages on different complex channels*.

As detailed in § 2.2, only a few works have previously attempted to characterize the performance of concurrent UWB communications over different complex channels experimentally. Flury et al. [24] have simulated the impact of multi-user interference (MUI) on energy detection-based UWB receivers. Vecchia et al. [62] have demonstrated the unreliability of concurrent transmissions over different complex channels on off-the-shelf UWB hardware, suggesting the use of a tight synchronization to improve performance. Our work builds on top of their observation, suggests additional enhancements that can be used in combination (or in absence) of a tight synchronization to significantly boost performance.

CFO across concurrent transmitters. Existing literature mentions that a large CFO across concurrent transmitters typically results in a fast beating pattern, which is deleterious for communication [5, 46]. These works, however, refer to concurrent transmissions within the same Glossy-based flood. Instead, we show that introducing a large CFO across independent concurrent transmitters allows to improve performance over different complex channels. In a prior poster abstract [52], we have laid out this idea. This paper validates this hypothesis with a thorough empirical validation, and proposes its concrete use (DETUNE), alongside with several other enhancements, analyzing their benefits and drawbacks.

10 CONCLUSION

This paper provides concrete methods enabling co-located UWB devices to reliably transmit data concurrently over different complex channels while retaining the ability to carry out cm-accurate ranging. In detail, we present and experimentally evaluate three tuning levers – namely the synchronization of transmissions, the optimization of PHY settings, and the detuning of the CFO among different transmitters – that can improve the separation of concurrent transmissions over different complex channels. We empirically show the effectiveness of the proposed methods (as well as their combinations), discussing both their advantages and drawbacks. We then show how the proposed tuning levers enable more than eight concurrent UWB transmissions on the same frequencies sustaining a PRR above 99 %, significantly advancing the state of the art. We also highlight how the accuracy and precision of concurrent ranging measurements is unaffected, i.e., our methods can be used to improve and scale up UWB systems while retaining their ability to carry out centimetre-accurate ranging. We believe that our findings will be crucial in enabling the design of robust UWB-based localization systems that scale to large areas and coexist with co-located systems.

ACKNOWLEDGMENTS

The authors would like to sincerely thank the anonymous shepherd and reviewers for their comments and feedback. This work has been performed within the SPiDR project ("Secure, Performant, Dependable, and Resilient Wireless Mesh Networks") financed by the Technology Innovation Institute. This work was also supported by the TU Graz LEAD project "Dependable Internet of Things in Adverse Environments".

REFERENCES

[1] ABIresearch. 2020. 2021 Will Be the Year Ultra-Wideband Will Emerges as a Key Wireless Connectivity Technology for Indoor Positioning. [Online] https://tinyurl.com/2s3ufv5r – Last access: 2024-06-30.

[2] Alireza Ansaripour, Milad Heydariaan, and Omprakash Gnawali. 2024. Link Characteristics Study of Ultra-Wideband Radios. *Ad Hoc Networks* 156 (April 2024).

[3] Alireza Ansaripour, Aryo Yarahmadi, Milad Heydariaan, and Omprakash Gnawali. 2023. RIC3: Reliability Improvement in UWB Networks Using Enhanced CCA and Complex Channels. In *2023 19th International Conference on Distributed Computing in Smart Systems and the Internet of Things (DCOSS-IoT)*. IEEE, 179–186.

[4] Michael Baddeley, Adnan Aijaz, Usman Raza, Aleksandar Stanoev, Yichao Jin, Markus Schuß, Carlo Alberto Boano, and George Oikonomou. 2021. 6TiSCH++ with Bluetooth 5 and Concurrent Transmissions. In *Proceedings of the 2021 International Conference on Embedded Wireless Systems and Networks*. 25–30.

[5] Michael Baddeley, Carlo Alberto Boano, Antonio Escobar-Molero, Ye Liu, Xiaoyuan Ma, Victor Marot, Usman Raza, Kay Römer, Markus Schuß, and Aleksandar Stanoev. 2023. Understanding Concurrent Transmissions: The Impact of Carrier Frequency Offset and RF Interference on Physical Layer Performance. *ACM Transactions on Sensor Networks* 20, 1 (June 2023).

[6] Andreas Biri, Neal Jackson, Lothar Thiele, Pat Pannuto, and Prabal Dutta. 2020. SociTrack: Infrastructure-Free Interaction Tracking through Mobile Sensor Networks. In *Proceedings of the 26th International Conference on Mobile Computing and Networking (MobiCom)*. ACM.

[7] Hannah Brunner, Michael Stocker, Maximilian Schuh, Markus Schuß, Carlo Alberto Boano, and Kay Römer. 2022. Understanding and Mitigating the Impact of Wi-Fi 6E Interference on Ultra-Wideband Communications and Ranging. In *Proceedings of the 21st International Conference on Information Processing in Sensor Networks (IPSN)*. IEEE.

[8] Tengfei Chang, Thomas Watteyne, Kris Pister, and Qin Wang. 2015. Adaptive synchronization in multi-hop TSCH networks. *Computer Networks* 76 (2015), 165–176.

[9] Tengfei Chang, Thomas Watteyne, Xavier Vilajosana, and Pedro Henrique Gomes. 2018. Constructive Interference in 802.15.4: A Tutorial. *IEEE Communications Surveys & Tutorials* 21, 1 (Sept. 2018), 217–237.

[10] Maximilien Charlier, Bruno Quoitin, and David Hauweele. 2019. Challenges in Using Time Slotted Channel Hopping with Ultra Wideband Communications. In *Proceedings of the 4th International Conference on Internet of Things Design and Implementation (IoTDI)*. ACM.

[11] Maximilien Charlier, Bruno Quoitin, and David Hauweele. 2019. UWB-TSCH: Time and Frequency Division Multiplexing for UWB Communications. In *Rencontres Francophones sur la Conception de Protocoles, l'Evaluation de Performance et l'Expérimentation des Réseaux de Communication (CoRes)*. [Online] https://hal.archives-ouvertes.fr/hal-02122611 – Last access: 2024-06-30.

[12] Dieter Coppens, Adnan Shahid, Sam Lemey, Ben Van Herbruggen, Chris Marshall, and Eli De Poorter. 2022. An Overview of UWB Standards and Organizations (IEEE 802.15.4, FiRa, Apple): Interoperability Aspects and Future Research Directions. *IEEE Access* 10 (June 2022).

[13] Pablo Corbalán and Gian Pietro Picco. 2020. Ultra-Wideband Concurrent Ranging. *ACM Transactions on Sensor Networks (TOSN)* 16, 4 (Sept. 2020), 1–41.

[14] Pablo Corbalán, Gian Pietro Picco, and Sameera Palipana. 2019. Chorus: UWB Concurrent Transmissions for GPS-like Passive Localization of Countless Targets. In *Proceedings of the 18th International Conference on Information Processing in Sensor Networks*. IEEE, 133–144.

[15] Decawave. 2016. *DW1000 Device Driver Application Programming Iinterface (API) Guide*. Technical Report Version 2.7.

[16] Decawave. 2018. APH010 DW1000 Inter-channel Interference: How Transmissions on one DW1000 Channel can Affect other Channels and how to Minimize that Effect, v1.1.

[17] Decawave. 2018. Battery Life Calculator For DW1000 in Two-Way Ranging Use Case. [Online] https://forum.qorvo.com/t/power-calculator-released – Last access: 2024-06-30.

[18] Decawave. 2018. DW1000 User Manual, v2.14.

[19] Decawave. 2021. DW3000 Family User Manual, v1.1.

[20] EETimes. 2019. VW and NXP Show First Car Using UWB To Combat Relay Theft. [Online] https://tinyurl.com/201ybh88y5e – Last access: 2024-06-30.

[21] Atis Elsts, Simon Duquennoy, Xenofon Fafoutis, George Oikonomou, Robert Piechocki, and Ian Craddock. 2016. Microsecond-Accuracy Time Synchronization using the IEEE 802.15.4 TSCH Protocol. In *Proceedings of the 41st International Conference on Local Computer Networks (LCN) Workshops*. IEEE, 156–164.

[22] European Union. 2019. Commission Implementing Decision (EU) 2019/785 of 14 May 2019 on the Harmonisation of Radio Spectrum for Equipment using Ultra-Wideband Technology in the Union and repealing Decision 2007/131/EC. [Online] https://tinyurl.com/4cbdefcm – Last access: 2024-06-30.

[23] Federico Ferrari, Marco Zimmerling, Lothar Thiele, and Olga Saukh. 2011. Efficient Network Flooding and Time Synchronization with Glossy. In *Proceedings of the 10th International Conference on Information Processing in Sensor Networks (IPSN)*. IEEE, 73–84.

[24] Manuel Flury, Ruben Merz, Jean-Yves Le Boudec, and Julien Zory. 2007. Performance Evaluation of an IEEE 802.15.4a Physical Layer with Energy Detection and Multi-user Interference. In *Proceedings of the IEEE International Conference on Ultra-Wideband (ICUWB)*. IEEE, 663–668.

[25] Markus Gallacher, Michael Stocker, Michael Baddeley, Kay Römer, and Carlo Alberto Boano. 2023. InSight: Enabling NLOS Classification, Error Correction, and Anchor Selection on Resource-Constrained UWB Devices. In *Proceedings of the 20th International Conference on Embedded Wireless Systems and Networks (EWSN)*. ACM, 132–144.

[26] Thomas Gigl, Florian Troesch, Josef Preishuber-Pfluegl, and Klaus Witrisal. 2012. Ranging Performance of the IEEE 802.15.4a UWB Standard under FCC/CEPT Regulations. *Journal of Electrical and Computer Engineering* (April 2012).

[27] Bernhard Großwindhager, Michael Rath, Josef Kulmer, Mustafa S Bakr, Carlo Alberto Boano, Klaus Witrisal, and Kay Römer. 2018. SALMA: UWB-based Single-Anchor Localization System using Multipath Assistance. In *Proceedings of the 16th International Conference on Embedded Networked Sensor Systems (SenSys)*. ACM, 132–144.

[28] Bernhard Großwindhager, Michael Stocker, Michael Rath, Carlo Alberto Boano, and Kay Römer. 2019. SnapLoc: An Ultra-Fast UWB-based Indoor Localization System for an Unlimited Number of Tags. In *Proceedings of the 18th International Conference on Information Processing in Sensor Networks (IPSN)*. IEEE, 61–72.

[29] Bernhard Großwindhager, Carlo Alberto Boano, Michael Rath, and Kay Römer. 2018. Enabling Runtime Adaptation of Physical Layer Settings for Dependable UWB Communications. In *Proceedings of the 19th International Symposium on a World of Wireless, Mobile and Multimedia Networks (WoWMoM)*. IEEE, 1–11.

[30] IEEE. 2007. 802.15.4a-2007: Standard for Information Technology – Specific Requirement Part 15.4: Wireless Medium Access Control (MAC) and Physical Layer (PHY) Specifications for Low-Rate Wireless Personal Area Networks (WPANs).

[31] IEEE. 2016. 802.15.4-2015: IEEE Standard for Low-Rate Wireless Networks.

[32] IEEE. 2020. 802.15.4-2020: IEEE Standard for Low-Rate Wireless Networks.

[33] IEEE. 2020. 802.15.4z-2020: IEEE Standard for Low-Rate Wireless Networks – Amendment 1: Enhanced Ultra Wideband (UWB) Physical Layers (PHYs) and Associated Ranging Techniques.

[34] IEEE P802.15 Working Group for Wireless Personal Area Networks (WPANs). 2023. Comparison of Ipatov Sequences of Different Lengths. Document no. IEEE 802.15-23/0050r0.

[35] V.P. Ipatov. 1979. Ternary Sequences with Ideal Periodic Autocorrelation Properties. *Radio Engineering and Electronic Physics* 24 (1979), 75–79.

[36] Timofei Istomin, Elia Leoni, Davide Molteni, Amy L. Murphy, Gian Pietro Picco, and Maurizio Griva. 2022. Janus: Dual-Radio Accurate and Energy-Efficient Proximity Detection. *ACM IMWUT* 5, 4 (Dec. 2022).

[37] Timofei Istomin, Amy L Murphy, Gian Pietro Picco, and Usman Raza. 2016. Data Prediction + Synchronous Transmissions = Ultra-Low Power Wireless Sensor Networks. In *Proceedings of the 14th International Conference on Embedded Network Sensor Systems (SenSys)*. ACM, 83–95.

[38] Avinash Kalyanaraman, Yunze Zeng, Sushanta Rakshit, and Vivek Jain. 2020. CaraoKey: Car States Sensing via the Ultra-Wideband Keyless Infrastructure. In *Proceedings of the 17th International Conference on Sensing, Communication, and Networking (SECON)*. IEEE, 1–9.

[39] Benjamin Kempke, Pat Pannuto, Bradford Campbell, and Prabal Dutta. 2016. SurePoint: Exploiting Ultra Wideband Flooding and Diversity to Provide Robust, Scalable, High-Fidelity Indoor Localization. In *Proceedings of the 14th International Conference on Embedded Network Sensor Systems (SenSys)*. ACM, 137–149.

[40] Anton Ledergerber, Michael Hamer, and Raffaello D'Andrea. 2015. A Robot Self-Localization System using One-Way Ultra-Wideband Communication. In *Proceedings of the International Conference on Intelligent Robots and Systems (IROS)*. IEEE / RSJ, 3131–3137.

[41] Diego Lobba, Matteo Trobinger, Davide Vecchia, Timofei Istomin, and Gian Pietro Picco. 2020. Concurrent Transmissions for Multi-hop Communication on Ultra-Wideband Radios. In *Proceedings of the 17th International Conference on Embedded Wireless Systems and Networks (EWSN)*. Junction Publishing, 132–143.

[42] Markets and Markets. 2020. Ultra-Wideband Market – Global Forecast to 2025. [Online] https://tinyurl.com/2p8cw386 – Last access: 2024-06-30.

[43] Hessam Mohammadmoradi and Omprakash Gnawali. 2019. Study and Mitigation of Non-Cooperative UWB Interference on Ranging. In *Proceedings of the 16th International Conference on Embedded Wireless Systems and Networks (EWSN)*. Junction Publishing, 142–153.

[44] Hessam Mohammadmoradi, Milad Heydariaan, and Omprakash Gnawali. 2018. UWB Physical Layer Adaptation for best Ranging Performance within Application Constraints. In *Proceedings of the 2nd International Conference on Smart Digital Environment (ICSDE)*. ACM.

[45] Hessam Mohammadmoradi, Milad Heydariaan, and Omprakash Gnawali. 2018. UWB Physical Layer Adaptation for Best Ranging Performance within Application Constraints. In *Proceedings of the 2nd International Conference on Smart Digital Environment (ICSDE)*. ACM, 119–126.

[46] Beshr Al Nahas, Antonio Escobar-Molero, Jirka Klaue, Simon Duquennoy, and Olaf Landsiedel. 2021. BlueFlood: Concurrent Transmissions for Multi-hop Bluetooth 5—Modeling and Evaluation. *ACM Trans. Internet Things* 2, 4 (July 2021).

[47] Nordic Semiconductor. 2017. nRF52832 Product Specification v1.4. [Online] https://infocenter.nordicsemi.com/pdf/nRF52832_PS_v1.4.pdf – Last access: 2024-06-30.

[48] NXP. 2021. SR040 Ultra-Wideband Transceiver – Product short data sheet, Rev. 1.2.

[49] NXP. 2021. SR150 Ultra-Wideband Transceiver – Product short data sheet, Rev. 1.0.

[50] Matteo Ridolfi, Samuel Van de Velde, Heidi Steendam, and Eli De Poorter. 2018. Analysis of the Scalability of UWB Indoor Localization Solutions for High User Densities. *MDPI Sensors* 18, 6 (June 2018).

[51] Samsung. 2020. Exynos Connect U100 – Connect to ultra-wide experiences. [Online] https://tinyurl.com/48cn85mm – Last access: 2024-06-30.

[52] Maximilian Schuh, Carlo Alberto Boano, and Kay Römer. 2022. Increasing the Reliability of Concurrent UWB Transmissions over Complex Channels. In *Proceedings of the 19th International Conference on Embedded Wireless Systems and Networks (EWSN), poster session.*

[53] Maximilian Schuh, Hannah Brunner, Michael Stocker, Markus Schuß, Carlo Alberto Boano, and Kay Römer. 2022. First Steps in Benchmarking the Performance of Heterogeneous Ultra-Wideband Platforms. In *Proceedings of the 5th International Workshop on Benchmarking Cyber-Physical Systems and Internet of Things (CPS-IoTBench)*. IEEE, 34–39.

[54] Petr Sedlacek, Martin Slanina, and Pavel Masek. 2019. An Overview of the IEEE 802.15.4z Standard its Comparison and to the Existing UWB Standards. In *Proceedings of the 29th International Conference Radioelektronika (RADIOELEKTRONIKA)*. IEEE, 1–6.

[55] Sewio Networks s.r.o. 2024. Asset Tracking and Material Flow Analysis in Real-time. [Online] https://www.sewio.net/indoor-asset-tracking-and-material-flow-analysis/ – Last access: 2024-06-30.

[56] Enrico Soprana, Matteo Trobinger, Davide Vecchia, and Gian Pietro Picco. 2023. Network On or Off? Instant Global Binary Decisions over UWB with Flick. In *Proceedings of the 22nd International Conference on Information Processing in Sensor Networks (IPSN)*. ACM, 261–273.

[57] David Stanislowski, Xavier Vilajosana, Qin Wang, Thomas Watteyne, and Kristofer SJ Pister. 2013. Adaptive synchronization in IEEE802. 15.4 e networks. *IEEE Transactions on Industrial Informatics* 10, 1 (2013), 795–802.

[58] Michael Stocker, Hannah Brunner, Maximilian Schuh, Carlo Alberto Boano, and Kay Römer. 2022. On the Performance of IEEE 802.15.4z-Compliant Ultra-Wideband Devices. In *Proceedings of the 5th International Workshop on Benchmarking Cyber-Physical Systems and Internet of Things (CPS-IoTBench)*. IEEE, 28–33.

[59] Bharath Sundararaman, Ugo Buy, and Ajay D. Kshemkalyani. 2005. Clock Synchronization for Wireless Sensor Networks: A Survey. *Ad Hoc Networks* 3, 3 (May 2005), 281–323.

[60] The FiRa Consortium. 2024. Technical FAQ. [Online] https://www.firaconsortium.org/resource-hub/technical-faq – Last access: 2024-06-30.

[61] Matteo Trobinger, Davide Vecchia, Diego Lobba, Timofei Istomin, and Gian Pietro Picco. 2020. One Flood to Route them All: Ultra-Fast Convergecast of Concurrent Flows over UWB. In *Proceedings of the 18th Conference on Embedded Networked Sensor Systems (SenSys)*. ACM, 179–191.

[62] Davide Vecchia, Pablo Corbalán, Timofei Istomin, and Gian Pietro Picco. 2019. Playing with Fire: Exploring Concurrent Transmissions in Ultra-Wideband Radios. In *Proceedings of the 16th International Conference on Sensing, Communication, and Networking (SECON)*. IEEE, 1–9.

[63] Wired. 2019. The Biggest iPhone News Is a Tiny New Chip Inside It. [Online] https://www.wired.com/story/apple-u1-chip/ – Last access: 2024-06-30.

[64] Yu Xianjia, Li Qingqing, Jorge Peña Queralta, Jukka Heikkonen, and Tomi Westerlund. 2021. Cooperative UWB-Based Localization for Outdoors Positioning and Navigation of UAVs aided by Ground Robots. In *Proceedings of the International Conference on Autonomous Systems (ICAS)*. IEEE, 1–5.

[65] Marco Zimmerling, Luca Mottola, and Silvia Santini. 2020. Synchronous Transmissions in Low-Power Wireless: A Survey of Communication Protocols and Network Services. *ACM Comput. Surv.* 53, 6 (Dec. 2020).